THE INFLUENCE OF FLOW PASSAGE GEOMETRY ON THE PERFORMANCES OF A SUPERCRITICAL CO_2 CENTRIFUGAL COMPRESSOR

by

Dong-Bo SHI [a], Yu-Qi WANG [b], Yong-Hui XIE [a*], and Di ZHANG [b]

[a] Shaanxi Engineering Laboratory of Turbomachinery and Power Equipment, School of Energy and Power Engineering, Xi'an Jiaotong University, Xi'an, China
[b] MOE Key Laboratory of Thermo-Fluid Science and Engineering, School of Energy and Power Engineering, Xi'an Jiaotong University, Xi'an, China

Original scientific paper
https://doi.org/10.2298/TSCI170731253S

In this paper, based on the thermodynamic design of the supercritical carbon dioxide (sCO_2) centrifugal compressor, the design idea of the flow passage geometries and the method to improve the performance of the sCO_2 centrifugal compressor are discussed. With the help of commercial software ANSYS CFX, the influence of the shape of the leading edge and trailing edge is studied, and the elliptical leading edge makes the pressure ratio 10.30% higher and the efficiency 3.95% higher than the square leading edge. By changing the forward-swept angle and backward-swept angle of the leading edge, the effects of aerodynamic swept shape in sCO_2 centrifugal compressor are discussed. The effect of the gap between the impeller blade and diffuser blade is discussed, and the 10 mm gap makes the performance best. The pressure ratio is increased by 2.5% compared with the original design, while at the same time the efficiency is slightly improved. In summary, based on thermal design of the sCO_2 centrifugal compressor, the effects of different flow geometries are analyzed in detail.

Key words: *centrifugal compressor, sCO_2, numerical simulation flow passage geometry influence*

Introduction

The centrifugal compressor has the characteristics of compact structure, good process performance and high single-stage pressure ratio, so that it plays an important role in aerospace and transportation. It has been widely used in various fields of industry. In aerospace industry the centrifugal compressor is mainly used in turboshaft and turboprop engines. The composition of the centrifugal compressor in the engine develops from single-stage centrifugal compressor, axial-flow and single stage centrifugal compressor to two stage centrifugal compressor, and there have been diagonal-flow compressor and diagonal-flow centrifugal compressor.

With the growing demand for development, there are higher requirements for structure and performance of centrifugal compressor. Meanwhile, the centrifugal compressor using normal refrigerant has been difficult to meet the design requirements. The CO_2 has become one of the

* Corresponding author, e-mail: yhxie@mail.xjtu.edu.cn

most promising natural refrigerants due to its characteristic properties under supercritical condition. The CO_2 is colorless, odorless and non-toxic. Besides, it has steady chemical properties and it is easy to get because it widely exists in the atmosphere. The critical temperature of CO_2 is 31.1 °C and critical pressure is 7.4 MPa [1], thus it is easy for CO_2 to reach the supercritical state, which has lower requirement on equipment and decrease the production cost. The CO_2 has high density like liquid, low viscosity like gas and low surface tension and has good flow, penetration and transfer performance under supercritical condition [2, 3]. Using sCO_2 as thermodynamic cycle refrigerant makes it possible to make full use of the characteristics of the high density near the critical point, reduce the compression power of the whole cycle [4] and improve cycle efficiency. Meanwhile, the compressor using sCO_2 as refrigerant has a smaller structure [5].

Based on the special characteristics of sCO_2, some scholars have carried out theoretical analysis, numerical simulation and experimental research on the design, parameter optimization and efficiency of sCO_2 centrifugal compressor. Kim [6, 7] analyzed the performance of sCO_2 centrifugal compressor with different mass-flow rate by numerical method and experimental method. It is found that the numerical simulation results are in good agreement with the experimental results. The sCO_2 compressor test system was constructed by Sandia National Laboratories Albuquerque, N. Mex., USA. The flow characteristics of the compressor and the system control near the critical point were studied by theoretical analysis and experimental measurement [5]. Pecnik *et al*. [8] used Spalart-Allmaras (S-A) model and two equation k-ω SST turbulence model to carry out the numerical analysis of the radial-flow sCO_2 compressor, and compared the numerical results with the sCO_2 compression cycle test data of Sandia National Laboratories. Ishizuka *et al*. [9] and Muto *et al*. [10] used a modular approach to design a small size centrifugal compressor as a test of the sCO_2 compressor together with their partners.

Based on the current research, this paper attempts to explore and excavate new design freedom, enrich and increase the design dimensions, expect to improve the working ability of sCO_2 centrifugal compressor. The pressure ratio and efficiency of the compressor can be further improved by changing the shape of the leading edge and trailing edge of the blade, the shape of the blade leading edge and the gap between the impeller and the vane diffuser.

Design of the sCO_2 compressor

The state parameters of inlet and outlet are selected by taking example from Zhao *et al.* [11]. The compressor design was developed using a three-step design process. First, a quick parametric screening study using mean line analysis and empiricism was conducted to synthesize the effects of various design parameters on performance [12]. Based on 1-D flow, the thermodynamic parameters of each feature point and the basic dimensions of the main parts of the flow passage are finally determined with the support of the actual gas state equation, process equation, flow continuity equation, momentum equation, and energy equation. Once a skeletal geometry model that had a performance potential consistent with the requirements was established by self-developed program. The detailed geometry of the centrifugal compressor was sculpted using ANSYS Workbench as a turbomachinery geometry modeler. The development of the detailed geometry was guided by various aerodynamic analysis tools including 3-D viscous CFD.

The performance estimates as well as the state parameters at inlet and outlet of the designed centrifugal compressor are listed in tab. 1. The detailed geometric parameters of the impeller and diffuser are determined in the design process. In this paper, multiple tests were conducted to ensure the high efficiency of the sCO_2 centrifugal compressor. Figure 1 shows the meridional planes shape of the impeller of the designed sCO_2 compressor and fig. 2 for the geometry of the diffuser.

Table 1. Performance estimates and state parameters of the designed compressor

Type	Parameters	Value
	Input power, [MW]	5
Performance estimates	Mass-flow rate, [kgs^{-1}]	272.6
	Rotational speed, [rpm]	15000
	Efficiency, [%]	79.5
	Inlet temperature, [K]	306.7
State parameters	Inlet pressure, [MPa]	8.96
	Outlet temperature, [K]	327.5
	Outlet pressure, [MPa]	18.94

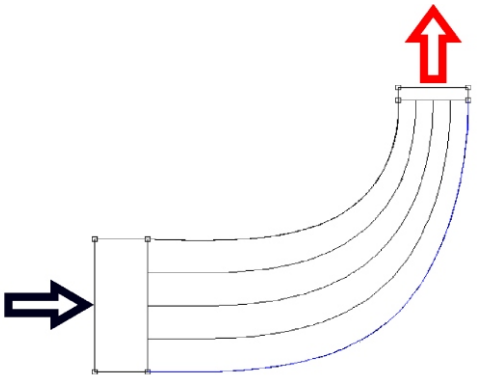

Figure 1. Meridional planes shape of the impeller

Figure 2. Meridional planes shape of the diffuser

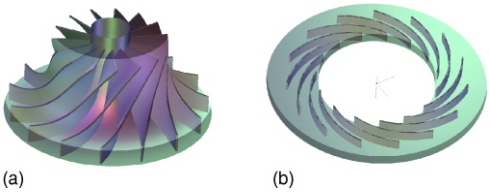

Figure 3. The sCO_2 centrifugal compressor 3-D model; (a) impeller, (b) diffuser

According to the geometric parameters of thermal design, the 3-D modeling of impeller and diffuser of sCO_2 centrifugal compressor is carried out, as shown in fig. 3. The whole 3-D model includes 15 impeller blades and 15 diffuser blades, the impeller radius is 101.959 mm, and impeller blade height at outlet is 18.586 mm.

Numerical methods

Boundary conditions

In this paper, a single passage model (a impeller flow passage and a diffuser flow passage) is adopted for numerical calculation. The refrigerant is sCO_2, and the physical parameters are the same with CO2RK in the MATERIAL-redkw database in ANSYS CFX. The database is based on the Redlich-Kwong equation, and provides a variety of amendments. Kim *et al*. [6] estimate the error between the real properties and the ones calculated within the CFX code to verify the reliability of the CO2RK. The boundary conditions of mass, flow, and temperature are given in the impeller fluid flow field, and the inlet flow rate is 18.173 kg/s, the inlet temperature is 306.7 K. Besides, the impeller fluid-flow, field is set around the Z axis with a rotational speed of 15000 rpm. The diffuser fluid-flow field is set as the pressure outlet boundary condition, and the outlet pressure is 18.94 MPa. The mixed model Frozen rotor is adopted to couple the flow of the impeller and diffuser. Meanwhile, the wall surface of the diffuser is set as an absolutely stationary wall, and the wall of the impeller is set as a relatively stationary wall, and the upper and the lower walls of all the regions are adiabatic walls, which can meet the requirements of non-slip flow conditions.

Turbulence model

The SST k-ω turbulence model is adopted in this paper, which was proposed by Menter [13] based on the k-ε and k-ω turbulence model. This model combines the advantages of the k-ε turbulence model and k-ω turbulence model. It not only overcomes the limitations of k-ε turbulence

model to simulate the wall region of low Reynolds number, but also overcomes the disadvantage that the k-ω turbulence model has a high requirement for grid quality, so it is efficient and accurate to simulate turbulent flow. Some other scholars [14-16] have also used the turbulence model in the analysis of centrifugal compressor, and obtained reasonable results.

The numerical computation in this paper is accomplished in commercial software CFX. The flow and temperature field are acquired by solving 3-D Navier-Stokes equation. The numerical computation is considered converged when the residuals of continuity equation, momentum equation and energy equation are all below 1 10^{-4} and the average inlet pressure and outlet temperature deviation of adjacent iteration step is less than 0.1%.

Table 2. Grid independence (design model)

Number of grids	Impeller inlet pressure, [MPa]	Diffuser outlet temperature, [°C]	Impeller torque, [Nm^{-1}]
100000	8.8510	329.502	224.225
200000	8.9159	329.078	220.928
400000	9.0466	328.304	215.733
700000	9.0485	328.203	215.478

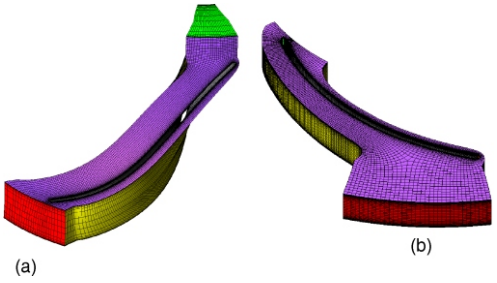

Figure 4. The schematic diagram of the mesh; (a) impeller flow passage, (b) diffuser flow passage

Grid dependence

This paper adopts hexahedral structured grid to mesh model, selecting the method of the combination of H-type, C-type, J-type, and L-type. The H-type meshing is used on the blade leading edge, trailing edge and side, and the O-type meshing is adopted on the blade surface. In order to avoid the calculation error caused by mesh precision, taking the design model as an example, a variety of grid scales (100000, 200000, 400000, and 700000) were used to measure the inlet pressure of the impeller, diffuser outlet temperature and impeller torque, and the verification results are shown in tab. 2. As can be seen from the table, the results of 400000 grids and the 700000 grids are relatively close. Taking into account the calculation of resources and time, the final selection of the number of the grid is about 400000. The schematic diagram of the mesh is shown in fig. 4.

Results and discussion

Different leading edge shapes

On the basis of the design model, the numerical simulation is carried out to study the effect of leading edge shape on sCO_2 centrifugal compressor. The calculation sets four programs, namely Square LE, Circle LE, Ellipse LE1, and Ellipse LE2, as is shown in fig. 5, where the elliptical axis ratio of Ellipse LE1 is 2.5 and that of Ellipse LE2 is 5. The trailing edges of the four programs are kept constantly circle, and the total chord length of the blades is consistent. Besides, the boundary conditions are the same as the design conditions.

Table 3 lists the comparison of performance parameters of centrifugal compressor with different leading edge shapes. It can be seen that the total pressure ratio of Ellipse LE2 is the largest and its efficiency is the best, followed by Ellipse LE1, Circle LE, and Square LE.

In this paper, the sCO_2 centrifugal compressor is evaluated by the total-total efficiency, and the concrete calculating methods are:

$$\eta_{T\ T} \quad \frac{h_{T_{\text{isout}}} \quad h_{T_{\text{in}}}}{h_{T_{\text{out}}} \quad h_{T_{\text{in}}}} \qquad (1)$$

where h is the represents the enthalpy value of sCO_2, in – the inlet of the centrifugal compressor, out – the outlet of the diffuser, T – the total parameters.

In the impeller passage, the fluid accelerates rapidly after bypassing the leading edge and over expands. When approaching the blade, a large inverse pressure gradient occurs on the blade surface due to the abrupt change of curvature, and the fluid tends to separate at this time. The disturbance of separation leads to the transition of laminar flow and downstream fluids undergo turbulent reattachment. Thus the separation bubble is formed. Figure 6 is streamline distributions of the impeller. As can be seen from fig. 6, for Square LE, separation bubbles are formed on both the suction and pressure side of the impeller blade, which are then re-absorbed on the blade surface downstream. Circle LE only produces a separation bubble on the suction side of the blade, and is rapidly adsorbed to the blade surface. The size of the separation bubble is much smaller than that of Square LE. Meanwhile, the loss near the trailing edge is much smaller. It is worth mentioning that the separation bubbles at the leading edge of Ellipse LE1 and Ellipse LE2 are very weak. Therefore, the loss of Ellipse LE is smaller than that of Circle LE.

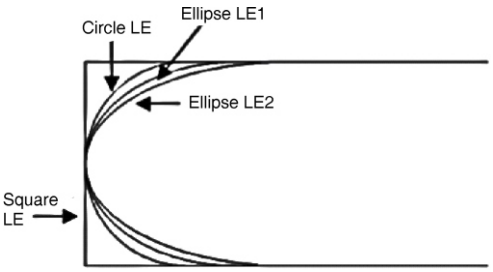

Figure 5. Different leading edge shapes

Table 3. The comparison of different leading edge shapes

Case	Power, [MW]	Total pressure ratio	Total-total efficiency
Square LE	4.613	1.872	0.7749
Circle LE	5.034	2.045	0.7802
Ellipse LE1	5.089	2.048	0.7858
Ellipse LE2	5.099	2.065	0.8055

Different trailing edge shapes

Similarly, on the basis of the design model, the numerical analysis of four different trailing edge shapes is carried out. Figure 7 shows the shape of the trailing edge enlargement, where the elliptical axis ratio of Ellipse TE1 is 2.5 and that of Ellipse TE2 is 5. Besides, the boundary conditions are the same as the design conditions.

Table 4 shows the comparison of performance parameters of centrifugal compressor with different trailing edge shapes. As can be seen from tab. 4, although the pressure ratio of the

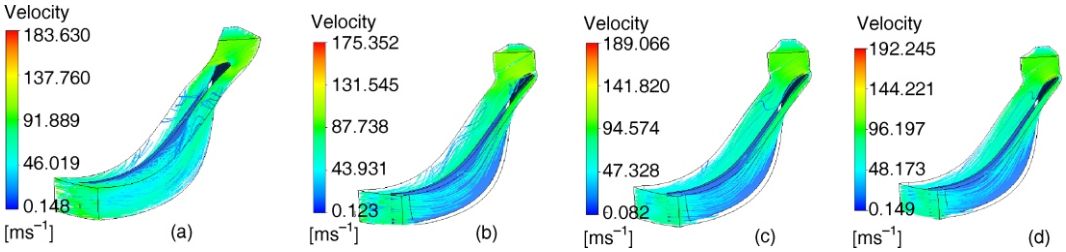

Figure 6. Streamline distributions of the impeller; (a) Square LE, (b) Circle LE, (c) Ellipse LE1, and (d) Ellipse LE2

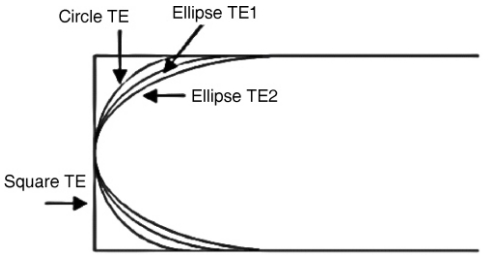

Figure 7. Different trailing edge shapes

Table 4. The comparison of different trailing edge shapes

Case	Power, [MW]	Total pressure ratio	Total-total efficiency
Square TE	5.248	2.109	0.7691
CircTE TE	5.081	2.049	0.7863
Ellipse TE1	5.019	2.045	0.7891
Ellipse TE2	5.132	2.059	0.7805

Square TE program is the highest, but the efficiency is the lowest, and the maximum efficiency difference with other programs is about 2%, which shows that the trailing edge of smooth transition is better than the blunt trailing edge. In addition, efficiency of Ellipse TE1 is higher than that of Ellipse TE2, while the total pressure ratio varies not much, which means that when the elliptical axis ratio is bigger, efficiency is not necessarily better.

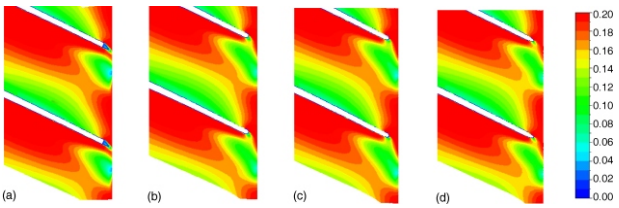

Figure 8. The relative Mach number distributions in 50% blade height section near the trailing edge; (a) Square LE, (b) Circle LE, (c) Ellipse LE1, and (d) Ellipse LE2

Figure 8 shows the relative Mach number distributions in 50% blade height section near the trailing edge. As can be seen, the impeller outlet flow uniformity of the Square TE scheme is relatively poor. Because the curvature of Square TE is large, the serious flow separation is occurred near leading edge region which in turn affects the flow in the diffuser. The increase of the non-uniformity of outlet flow leads to a large loss of the compressor, which shows that the efficiency is lower than the other three schemes. The difference between the relative Mach number distributions of the other schemes is very small, so the smooth shape of the trailing edge has little influence on the flow structure. At the same time, the bigger elliptical axis ratio of Ellipse TE will increase the Much number of the trailing edge which leading to a higher loss coefficient. So that the performance of Ellipse TE with smaller elliptical axis ratio is better.

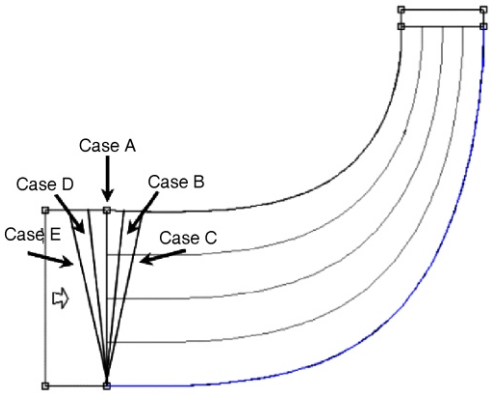

Figure 9. Different swept shape cases

Different leading edge swept shapes

In this paper, the numerical simulation of the different leading edge swept shapes of the centrifugal impeller is carried out based on the design model. Different schemes were recorded as Case A, Case B, Case C, Case D, and Case E, as shown in fig. 9. Among them, Case A is a normal blade whose leading edge is not swept. Case B and Case C are blades with backward-swept leading edges, whose backward-swept angles are 5° and 10°, respectively. Case D and Case E

are blades with forward-swept leading edges, whose forward-swept angles are 5° and 10°, respectively.

Table 5. The comparison of different leading edge swept shapes

Case	Power, [MW]	Total pressure ratio	Total-total efficiency
Case A	5.081	2.049	0.7863
Case B	5.071	2.052	0.7862
Case C	5.077	2.054	0.7850
Case D	5.076	2.048	0.7859
Case E	5.140	2.050	0.7799

Table 5 shows the effect of different leading edge sweeping shapes on the performance of sCO_2 centrifugal compressor. The total pressure ratio of the backward-swept leading edge is a little bit bigger than that of normal leading edge, but the efficiency of the backward-swept leading edge is lower than that of normal leading edge. When the backward-swept angle increases, the efficiency decreases, and the tendency of performance degradation increases. In addition, forward-swept leading edge has essentially the same total pressure ratio and a lower efficiency compared with normal leading edge. When the forward-swept angle increases, the efficiency decreases but the amplitude increases, and the tendency of performance degradation increases.

The static pressure distributions of meridional plane of different cases are shown in fig. 10. It can be found that the static pressure distributions at the inlet of the channel are obviously different. Relative to Case A, the low pressure ranges of the leading edges of Case B and Case C increase, and their pressure boost positions on the leading edges move rearward, the static pressure distributions are more uniform from the root to the top. The low pressure ranges of Case C and Case D are smaller than Case A, the static pressure distribution uniformity becomes worse and the pressure increase position moves forward at the top of the blade.

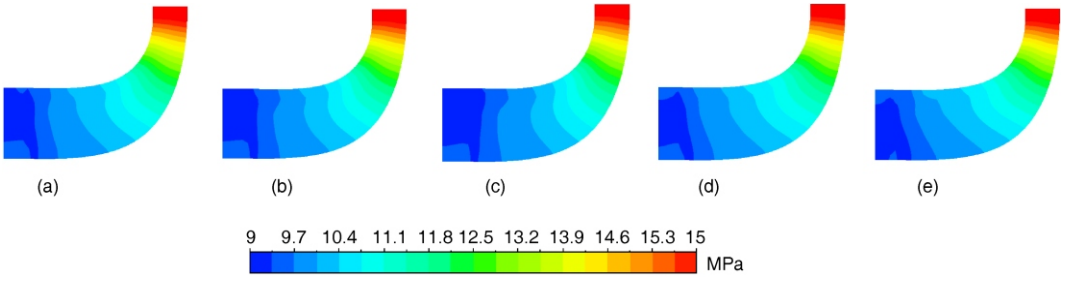

Figure 10. The static pressure distributions of meridional plane; (a) Case A, (b) Case B, (c) Case C, (d) Case D, and (e) Case E

Different gaps between diffuser and impeller

Based on the design model, varied gaps ($r_3 - r_2$) are adopted to study the effect on the performance of sCO_2 centrifugal compressor, as shown in fig. 11.

Table 6 shows the comparison of performance parameters of sCO_2 centrifugal compressor with different gaps between impeller blades and diffuser blades. As can be seen from the table, when the gap is 10 mm, the pressure ratio reaches the maximum, and the efficiency is high. When the gap is less than 10 mm, the pressure ratio and efficiency decrease with the decrease of the gap. Compared with gap 10 mm, although the efficiency of gap 12 mm is increased by 0.5%, but the pressure ratio is reduced by 1.3%, which shows that a larger gap does not necessarily lead to better performance.

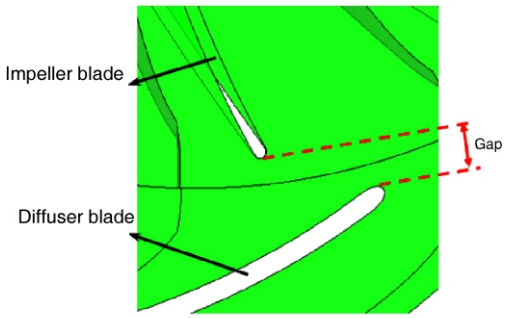

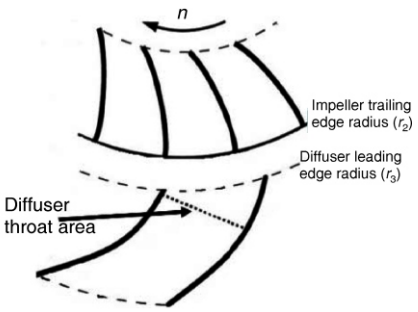

Figure 11. The impeller-diffuser geometry

Table 6. The comparison of different gaps

Case	Power, [MW]	Total pressure ratio	Total-total efficiency
4 mm	5.272	1.997	0.7533
6 mm	5.130	2.045	0.7840
8 mm	5.081	2.049	0.7863
10 mm	4.986	2.074	0.7864
12 mm	4.901	2.047	0.7904

Figure 12 shows the streamline distributions of blade-to-blade plot with five different gaps. It can be seen that when the gap is less than 8 mm, there is a vortex near the trailing edge of the suction side of the diffuser blade caused by flow separation. The vortex increases as the gap decreases, which greatly reduces the compressor performance.

On the other hand, in this paper, Mach number is less than 1, decreasing the radial gap size leads to a reduction in the diffuser throat area. Thus, it will lead to an increase in the flow velocity value and Much number at the leading edge of the diffuser. According to the total skin friction drag force, eq. (2), an increase in fluid velocity leads to an increment in the friction drag force, resulting in an increase in pressure drop. Therefore, a larger tip-speed Mach number have a higher loss coefficient and a lower pressure ratio for the compressor:

$$F \quad C_{\mathrm{f}} \frac{\rho_{\mathrm{f}} u^2}{2} S_{\mathrm{wetted}} \tag{2}$$

where ρ_{f} is the fluid density, u – the fluid velocity, S_{wetted} – the total surface area that is in contact with the fluid, and C_{f} – the Schlichting empirical formula that states turbulent flow is driven by the equation:

$$C_{\mathrm{f}} \quad \frac{0.455}{\log(\mathrm{Re})^{2.58}} \tag{3}$$

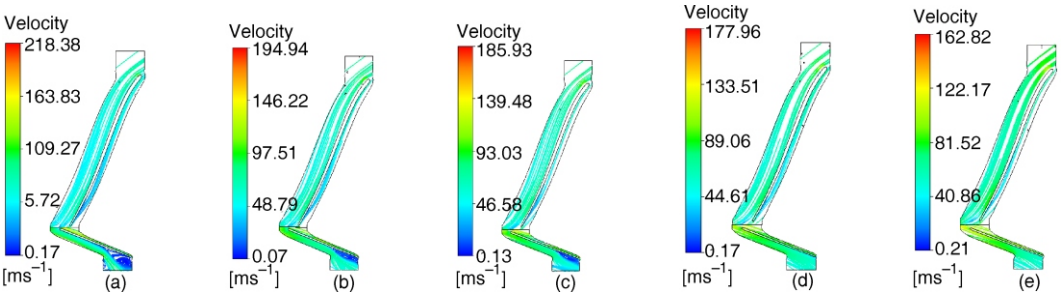

Figure 12. Streamline distributions of B2B; (a) gap 4 mm, (b) gap 6 mm, (c) gap 8 mm, (d) gap 10 mm, and (e) gap 12 mm

It also can be found by increasing the gap to 10 mm, the efficiency slightly increases but the pressure ratio significantly decreases. Because the space in the region of the diffuser leading edge increases, leading to increment of the mixing of non-uniform flow. Therefore, too large radial gap may have a higher loss.

Conclusions

In this paper, based on the 1-D thermal design, the design of SCO_2 centrifugal compressor flow geometry is carried out by a three-step design process. The methods to improve the performance are discussed by numerical calculations. Besides, the flow characteristics and compressor performance under different flow geometries are analyzed, the conclusions are as follows.

The loss of flow separation caused by Circular LE is smaller than that of Square LE, while Circular LE will also reduce the wake loss, so that the efficiency is improved. Ellipse LE will reduce the loss further. Ellipse LE makes the pressure ratio 10.30% higher and efficiency 3.95% higher than Square LE.

Ellipse TE will reduce the flow separation near the trailing edge region and increase the uniformity of outlet flow. The bigger elliptical axis ratio of Ellipse TE will increase the Much number of the trailing edge which leading to a higher loss coefficient, so Ellipse TE with smaller elliptical axis ratio is better. The elliptical trailing edge makes the efficiency at most 2% higher than the square leading edge.

The different leading edge sweep types can not significantly improve compression ratio, but will reduce efficiency and increase the blade manufacturing and installation difficulty.

The increase of gap will reduce the vortex caused by flow separation near the trailing edge of impeller and the friction drag force. At the same time, it will also increase of the mixing of non-uniform flow, therefore, too large radial gap may have a higher loss. The 10 mm gap achieves the best performance in this paper while the pressure ratio is increased by 2.5% compared with the original design and the efficiency is slightly improved.

Nomenclature

C_f – the Schlichting empirical formula
h – enthalpy, [Jkg^{-1}]
S_{wetted} – total surface area in contact with the fluid
u – fluid velocity

Greek symbols

η_{T-T} – total-total efficiency
ρ_f – fluid density

References

[1] Dostal, V., *et al.*, High-Performance Supercritical Carbon Dioxide Cycle for Next-Generation Nuclear Reactors, *Nuclear Science & Technology, 154* (2006), 3, pp. 265-282
[2] Tanaka, H., *et al.*, Forced Convection Heat Transfer to Fluid near Critical Point Flowing in Circular Tube, *International Journal of Heat & Mass Transfer, 14* (1971), 6, pp. 739-750
[3] Brassington, D. J., Cairn, D. N., Measurements of Forced Convective Heat Transfer to Supercritical Helium, *International Journal of Heat & Mass Transfer, 20* (1977), 3, pp. 207-214
[4] Wright, S. A., *et al*., Supercritical CO_2 Direct Cycle Gas Fast Reactor (SC-GFR) Concept, *Proceedings*, ASME 2011 Small Modular Reactors Symposium, American Society of Mechanical Engineers, Washington, DC, 2011
[5] Wright, S. A., *et al*., Operation and Analysis of a Supercritical CO_2 Brayton Cycle, Sandia Report 2010-0171, Sandia National Laboratorie, Albuquerque, N. Mex., USA, 2010
[6] Kim, S. G., *et al*., CFD Investigation of a Centrifugal Compressor Derived from Pump Technology for Supercritical Carbon Dioxide as a Working Fluid, *Journal of Supercritical Fluids, 86* (2014), Feb., pp. 160-171

[7] Kim, S. G., *et al*., Numerical Investigation of a Centrifugal Compressor for Supercritical CO_2 as a Working Fluid, *Proceedings*, ASME Turbo Expo 2014: Turbine Technical Conference and Exposition, Dusseldorf, Germany, 2014
[8] Pecnik, R., *et al*., Computational Fluid Dynamics of a Radial Compressor Operating with Supercritical CO_2, *Journal of Engineering for Gas Turbines and Power, 134* (2012), 12, pp. 201-213
[9] Ishizuka, T., *et al*., Design and Test Plan of the Supercritical CO_2 Compressor Test Loop, *Proceedings*, 16th International Conference on Nuclear Engineering, Orlando, Fla., USA, 2008
[10] Muto, Y., *et al*., Design of Small Centrifugal Compressor Test Model for a Supercritical CO_2 Compressor in the Fast Reactor Power Plant, *Proceedings*, ICAPP 08, Anaheim, Cal., USA, 2008
[11] Zhao, H., *et al*., Numerical Investigation on the Blade Tip Two-Phase Flow Characteristics of a Supercritical CO2 Centrifugal Compressor, *Journal of Engineering Thermophysics, 36* (2015), July, pp. 1433-1436
[12] Li, P. Y., *et al*., A New Optimization Method for Centrifugal Compressors Based on 1d Calculations and Analyses, *Energies, 8* (2015), 5, pp. 4317-4334
[13] Menter, F. R., Two-Equation Eddy-Viscosity Turbulence Models for Engineering Applications, *Aiaa Journal, 32* (1994), 8, pp. 1598-1605
[14] Mojaddam, M., *et al*., Experimental and Numerical Investigations of Radial Flow Compressor Component Losses, *Journal of Mechanical Science and Technology, 28* (2014), 6, pp. 2189-2196
[15] Nili-Ahmadabadi, M., *et al*., Investigation of a Centrifugal Compressor and Study of the Area Ratio and TIP Clearance Effects on Performance, *Journal of Thermal Science, 17* (2008), 4, pp. 314-323
[16] Mangani, L., *et al*., Assessment of Various Turbulence Models in a High Pressure Ratio Centrifugal Compressor with an Object Oriented CFD Code, *Journal of Turbomachinery, 134* (2012), 6, pp. 2219-2229

Paper submitted: July 31, 2016
Paper revised: January 11, 2017
Paper accepted: January 11, 2017

© 2018 Society of Thermal Engineers of Serbia.
Published by the Vinča Institute of Nuclear Sciences, Belgrade, Serbia.
This is an open access article distributed under the CC BY-NC-ND 4.0 terms and conditions.